

# Determination of Binary Diffusion Coefficients of Gases Using Holographic Interferometry in a Loschmidt Cell<sup>1</sup>

J. Baranski,<sup>2</sup> E. Bich,<sup>2</sup> E. Vogel,<sup>2,3</sup> and J. K. Lehmann<sup>2</sup>

---

A measuring system for the determination of binary diffusion coefficients of gases has been developed. The lower and upper half cells of the Loschmidt diffusion cell are fixed, one upon the other, contrary to the usual shearing cells. A sliding component between the half cells is moved to connect them and to start the diffusion. The concentration changes due to diffusion are determined by the optical method of real-time holographic interferometry. In this way the concentration is obtained as a function of time and location resulting from the analysis of the interference pattern. The data are evaluated by using the integrated diffusion equation for the closed-tube technique. First, measurements on the system argon-propane have been successfully performed at 1 bar and at room temperature. The results show an uncertainty of 1 per cent and are in good agreement with data by Wakeham and Slater (1974). Furthermore, refractive index measurements on the pure gases, argon and propane, as a function of gas density have been performed and evaluated to derive values of the first refractivity virial coefficient.

---

**KEY WORDS:** argon-propane; binary diffusion coefficient; closed-tube technique; gas mixtures; Loschmidt diffusion cell; measurement.

## 1. INTRODUCTION

A knowledge of transport properties is of great interest for engineering, environmental, and theoretical applications. Unfortunately, the precision

---

<sup>1</sup> Paper presented at the Sixteenth European Conference on Thermophysical Properties, September 1–4, 2002, London, United Kingdom.

<sup>2</sup> Universität Rostock, Fachbereich Chemie, Albert-Einstein-Str. 3a, D-18059 Rostock, Germany.

<sup>3</sup> To whom correspondence should be addressed. E-mail: eckhard.vogel@chemie.uni-rostock.de

of diffusion measurements is usually less than that of other transport properties like viscosity and thermal conductivity. Nevertheless, high accuracy has been claimed by most authors for their measurements. But the data obtained for the same system often differ greatly. One of the most reliable methods to determine binary diffusion coefficients of gases is the closed-tube method applying a Loschmidt cell [1–4]. In the present work a new Loschmidt cell alternative to the usual shearing cells has been developed and combined with holographic interferometry as a noninvasive, optical method for the determination of concentration changes due to diffusion. Unlike simple interferometry, the observation of an extended cell region is possible so that the concentration can be obtained as a function of time and location. A description of the theory basic to the measurements, the experimental setup, and the first results on the test system  $\text{Ar} + \text{C}_3\text{H}_8$  are given.

## 2. MEASURING THEORY

### 2.1. Diffusion

The mutual isochoric and isothermal concentration diffusion is an irreversible transport process characterized by a mutual flux of the chemical species and a decrease of the concentration gradient.

The continuity equation, neglecting source and sink terms, can be formulated for component  $i$  in the case of one-dimensional diffusion as

$$\frac{\partial \rho_i}{\partial t} = \frac{\partial D_{ij}}{\partial z} \frac{\partial \rho_i}{\partial z} + D_{ij} \frac{\partial^2 \rho_i}{\partial z^2} - w \frac{\partial \rho_i}{\partial z} - \rho_i \frac{\partial w}{\partial z} \quad i, j = 1, 2 \quad i \neq j \quad (1)$$

with

$$w(z, t) = \frac{1}{\rho} (\rho_i v_i + \rho_j v_j) \quad (2)$$

Here  $w$  is the average molar velocity,  $\rho_i$  and  $\rho_j$  are the molar densities of the components  $i$  and  $j$ ,  $\rho$  is that of the mixture, and  $D_{ij}$  is the binary diffusion coefficient.

Neglecting the concentration dependence of the diffusion coefficient and assuming a zero average molar velocity, Fick's second law follows immediately:

$$\frac{\partial \rho_i}{\partial t} = D_{ij} \frac{\partial^2 \rho_i}{\partial z^2} \quad (3)$$

This differential equation is to be solved for the boundary and initial conditions of the experimental method applied.

A general scheme of the closed-tube method using a Loschmidt cell of length  $L$  is shown in Fig. 1. The cell is initially separated into two half cells at position  $z = 0$ . The half cells are usually filled with two different pure gases. After connecting the half cells, the diffusion starts and the composition changes as a function of time and position throughout the cell. Taking into account the following initial and boundary conditions (subscript t, top and subscript b, bottom of the whole cell),

$$\begin{aligned}\rho_i(z, 0) &= \rho_{it} & 0 < z < L/2 \\ \rho_i(z, 0) &= \rho_{ib} & -L/2 < z < 0 \\ \frac{\partial \rho_i}{\partial z} &= 0 & \text{at } z = -L/2; z = L/2\end{aligned}$$

and the integration of Fick's second law leads to [3, 5]

$$\rho_i^{\text{id}}(z, t) = \rho_i^{\text{m}} - \frac{2}{\pi} \rho_i^{\text{d}} F^{(0)}(z, t) \quad (4)$$

with

$$F^{(0)}(z, t) = \sum_{k=0}^{\infty} \frac{e^{-(2k+1)^2 t/\tau}}{2k+1} \sin \frac{(2k+1)\pi z}{L} \quad (5)$$

$$\rho_i^{\text{m}} = (\rho_{ib} + \rho_{it})/2, \quad \rho_i^{\text{d}} = \rho_{ib} - \rho_{it}, \quad \tau = \frac{L^2}{\pi^2 D_{ij}} \quad (6)$$

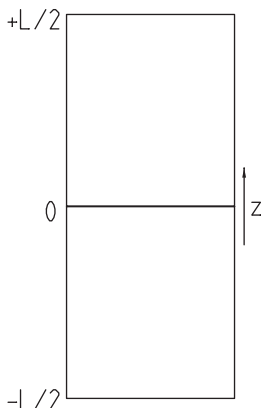


Fig. 1. Loschmidt cell.

The solution  $\rho_i^{\text{id}}$  corresponds to the ideal solution without corrections resulting from perturbation effects. Such effects can be caused by sources or sinks of the chemical species (due to desorption or absorption of the gases in the grease usually used for moving the half cells), by changes of the average molar velocity (due to the excess volume effect of real gases), and by the concentration dependence of  $D_{ij}$ . Furthermore, convection can be created by the movement of the sliding component in the middle of the cell to start the diffusion (see Section 3.1).

## 2.2. Holographic Interferometry

The determination of the concentration changes is carried out by holographic interferometry in real time (Kreis [6]). This method is based on the superposition of two wave fields. If the reference (index 1) and the object (index 2) waves are considered as transversal electromagnetic waves plane-polarized and with constant circular frequency  $\omega$  and constant wavelength  $\lambda$ , their electric field strengths  $E_i$  as a function of the position vector  $\mathbf{r}$  and of the time  $t$  can be formulated as

$$E_1(\mathbf{r}, t) = E_{01} e^{i(\mathbf{k}_1 \cdot \mathbf{r} - \omega t + \varphi_1)} \quad (7)$$

$$E_2(\mathbf{r}, t) = E_{02} e^{i(\mathbf{k}_2 \cdot \mathbf{r} - \omega t + \varphi_2)} \quad (8)$$

Here  $\mathbf{k}_i$  are the wave number vectors,  $E_{0i}$  are the amplitudes, and  $\varphi_i$  are the phases. When the waves interfere, a pattern results which is characterized by the intensity distribution:

$$I(\mathbf{r}, t) = (E_{01} - E_{02})^2 + 4E_{01}E_{02} \cos^2(\mathbf{k}' \cdot \mathbf{r} + \Delta\varphi) \quad (9)$$

with

$$\mathbf{k}' = \frac{\mathbf{k}_1 - \mathbf{k}_2}{2} \quad \Delta\varphi = \frac{\varphi_1 - \varphi_2}{2} \quad (10)$$

This pattern is recorded as a hologram. In order to reconstruct the original object wave, the hologram is again illuminated by the reference wave. In this procedure the reference wave is modulated by an amplitude transmission resulting in three contributions, one of which corresponds to the original object wave multiplied by a pure intensity term.

The object wave holographically reconstructed and the current object wave resulting as a consequence of alterations of the object can be characterized by the following relationships:

$$E_r(\mathbf{r}, t) = E_{0r} e^{i[\mathbf{k}_2 \cdot \mathbf{r} - \omega t + \varphi_2]} \quad (11)$$

$$E_c(\mathbf{r}, t) = E_{0c} e^{i[\mathbf{k}_2 \cdot \mathbf{r} - \omega t + \varphi_2 + \Delta\phi(\mathbf{r}, t)]} \quad (12)$$

Here the indices  $r$  and  $c$  denote the reconstructed and the current object waves. If the current object wave is superimposed on the reconstructed object wave in our experimental setup,  $\Delta\phi(\mathbf{r}, t)$  corresponds to the variable change of the phase distribution as a function of position and time due to diffusion. Under the assumption that the diffusion takes place only in one direction  $z$ , the superposition produces an interference pattern with the following intensity distribution:

$$I(z, t) = E_{01}^2 + E_{02}^2 + 2E_{01}E_{02} \cos[\Delta\phi(z, t)] \quad (13)$$

The difference  $\Delta\phi(z, t)$  caused by the change of the refractive index distribution  $\Delta n(y, z, t)$  in the transparent cell during the diffusion is given by

$$\Delta\phi(z, t) = \frac{2\pi}{\lambda} \Delta L(z, t) = \frac{2\pi}{\lambda} \int \Delta n(y, z, t) ds \quad (14)$$

with

$$\Delta n(y, z, t) = n(y, z, t) - n_0 \quad (15)$$

Here  $s$  is the coordinate of the optical path along the  $y$  direction in which the object wave moves through the cell of width  $l$ . The refractive index at  $t = 0$  is  $n_0$  and spatially constant.  $\Delta L(z, t)$  is the difference between the optical path lengths of reconstructed and current object waves and is responsible for the formation of the interference pattern. Finally, its minima for an ideal optical path length are given by

$$n(z, t) - n_0 = \left(k + \frac{1}{2}\right) \frac{\lambda}{l} \quad k = 0, 1, 2, \dots \quad (16)$$

In order to make use of holographic interferometry, the gases of the mixture under investigation (see below) must differ sufficiently in refractive indices. One essential advantage using holographic interferometry is that information obtained by the experiment does not only include data about the concentration at a fixed position, but additionally the local positions of certain concentrations at different times. This additional information is to be used for the evaluation of the diffusion coefficient as a function of concentration.

### 2.3. Determination of Molar Refraction

For the determination of the diffusion coefficient using the method of holographic interferometry, it is necessary to know the refractive indices of the pure gases as a function of density. For the mixture under investigation, such values are reported in the literature, e.g., by Kerl and Häusler [7]. But with consideration of future measurements on mixtures for which no literature data are available, the experimental setup was also applied to determine the refractive indices of the pure components in additional experiments. These measurements are based on the determination of the difference in the optical path length  $\Delta L(p)$  or the phase difference  $\Delta\phi(p)$  for a constant temperature  $T$  at a certain pressure  $p$  of the corresponding gas compared with that at  $p = 0$ .

For real gases the molar refraction  $R_i$  is given by the Lorentz–Lorenz equation:

$$R_i(\lambda) = \frac{n_i^2 - 1}{n_i^2 + 2} \rho_i^{-1} = \mathcal{A}_i + \mathcal{B}_{ii}\rho_i + \mathcal{C}_{iii}\rho_i^2 + \dots \quad (17)$$

Here  $\mathcal{A}_i$ ,  $\mathcal{B}_{ii}$ ,  $\mathcal{C}_{iii}$ ,... are the first, second, third,... refractivity virial coefficients.

In the refractive index measurements a current object wave changing its optical path length with the gas pressure in the cell is superimposed on an object wave reconstructed at the pressure  $p = 0$ . If any hologram is repositioned and illuminated with the reference wave at  $p = 0$ , an object wave  $E_r$  is reconstructed which is characterized by

$$E_r = E_{0r} e^{i[\phi_r(p=0)]} \quad (18)$$

The current object wave  $E_c$  corresponding to different filling pressures of the cell is given by

$$E_c = E_{0c} e^{i[\phi_c(p)]} \quad (19)$$

Both phases  $\phi_r(p = 0)$  and  $\phi_c(p)$  are independent of the coordinate  $z$ . The interference of the reconstructed and current object waves is characterized by the intensity,

$$I(p) = E_{0r}^2 + E_{0c}^2 + 2E_{0r}E_{0c} \cos[\Delta\phi(p)] \quad (20)$$

which is spatially constant and changes monotonically with increasing pressure. Here the phase difference  $\Delta\phi$  consists of the difference between

the optical path lengths of the reconstructed and current object waves and a constant small phase difference  $\varphi$ ;

$$\Delta\phi(p) = \frac{2\pi}{\lambda} \Delta L(p) + \varphi = \frac{2\pi}{\lambda} [n_i(p) - n(p=0)] l + \varphi \quad (21)$$

Taking into account  $n_i(p=0) = 1$ , the minima are described by

$$n_i(p) - 1 = \left(k + \frac{1}{2}\right) \frac{\lambda}{l} + \delta \quad k = 0, 1, 2, \dots \quad (22)$$

with

$$\delta = \frac{\varphi\lambda}{2\pi l} \quad (23)$$

$\delta$  is to be adjusted in the evaluation of the interference patterns in which a power series is fitted to  $n_i(p) - 1$ :

$$n_i(p) - 1 = \delta + \sum_{k=1}^m a_k \rho_{\text{id},i}^k \quad (24)$$

Here  $\rho_{\text{id},i} = p/(RT)$  is the ideal gas density and  $R$  is the universal gas constant.

## 2.4. Determination of Concentration

The virial equation of state and the Lorentz-Lorenz equation rewritten for the refractive index are given for each of the pure components  $i$  as

$$\frac{p}{RT} = \rho_i + B_{ii}\rho_i^2 + C_{iii}\rho_i^3 + \dots \quad (25)$$

$$\frac{n_i^2 - 1}{n_i^2 + 2} = \mathcal{A}_i\rho_i + \mathcal{B}_{ii}\rho_i^2 + \mathcal{C}_{iii}\rho_i^3 + \dots = R_i\rho_i \quad (26)$$

Here  $B_{ii}$  and  $C_{iii}$  are the second and third pressure virial coefficients. If the half cells are filled with pure components, the refractive index  $n_{0i}$  at the start of the diffusion in each of the half cells is related to the initial density  $\rho_{0i}$  (that means to  $\rho_{ib}$  or  $\rho_{it}$ ) by

$$n_{0i} = \left(\frac{1 + 2R_i\rho_{0i}}{1 - R_i\rho_{0i}}\right)^{1/2} \quad (27)$$

The equivalent equations for a binary mixture can be formulated as

$$\frac{P}{RT} = \rho_i + \rho_j + B_{ii}\rho_i^2 + 2B_{ij}\rho_i\rho_j + B_{jj}\rho_j^2 + C_{iii}\rho_i^3 + 3C_{iij}\rho_i^2\rho_j + 3C_{ijj}\rho_i\rho_j^2 + C_{jjj}\rho_j^3 + \dots \quad (28)$$

$$\frac{n_{\text{mix}}^2 - 1}{n_{\text{mix}}^2 + 2} = \mathcal{A}_i\rho_i + \mathcal{A}_j\rho_j + \mathcal{B}_{ii}\rho_i^2 + 2\mathcal{B}_{ij}\rho_i\rho_j + \mathcal{B}_{jj}\rho_j^2 + \mathcal{C}_{iii}\rho_i^3 + 3\mathcal{C}_{iij}\rho_i^2\rho_j + 3\mathcal{C}_{ijj}\rho_i\rho_j^2 + \mathcal{C}_{jjj}\rho_j^3 + \dots \quad (29)$$

Here the mixture virial coefficients are expressed by the corresponding interaction virial coefficients. In case that the second interaction virial coefficients are not available, they can reasonably be estimated by

$$B_{ij} = \frac{1}{2}(B_{ii} + B_{jj}) \quad (30)$$

$$\mathcal{B}_{ij} = (\mathcal{B}_{ii}\mathcal{B}_{jj})^{1/2} \quad (31)$$

The time-dependent interference patterns during the diffusion recorded by the CCD camera (see Fig. 2) shows an intensity distribution with maxima and minima visible as bright and dark horizontal lines. The refractive index  $n_{\text{mix}}(z, t)$  for the interference minimum  $k$  at the time  $t$  is

$$n_{\text{mix}}(z, t) = n_{0i} + \left(k + \frac{1}{2}\right) \frac{\lambda}{l} \quad (32)$$

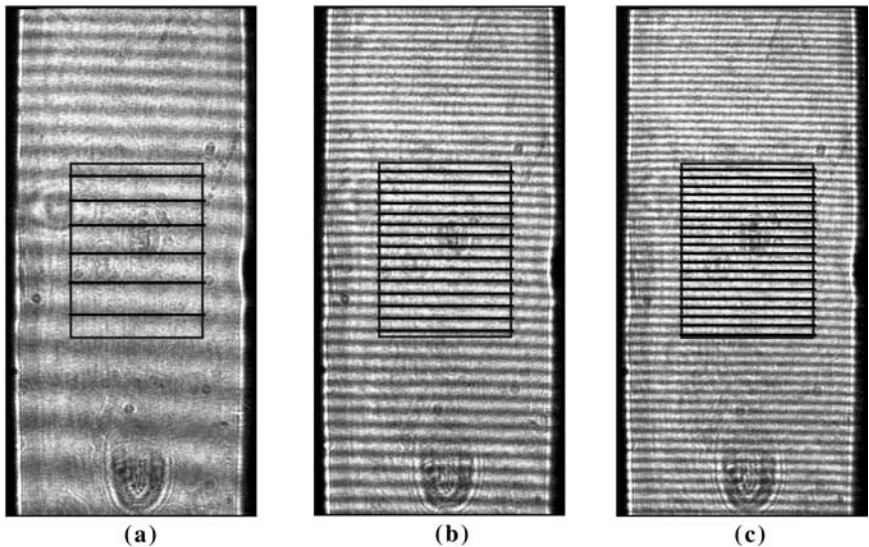


Fig. 2. Interference patterns at (a) the beginning, (b) the intermediate, and (c) the further course of a diffusion experiment.



At minimum, values of the pressure and refractivity virial coefficients for the pure gases are needed to obtain the molar concentrations  $\rho_i$  and  $\rho_j$  in the fitting process of the nonlinear Eqs. (28) and (29) to the measured data  $p$ ,  $T$ , and  $n_{\text{mix}}$ . Finally, Eq. (4) including Eqs. (5) and (6) are fitted to the molar densities of the components to determine the diffusion coefficient as the product of  $D_{ij}$  and  $\rho$ .

### 3. EXPERIMENTAL

#### 3.1. Loschmidt Diffusion Cell

The Loschmidt diffusion cell developed in this work is shown in Fig. 3. The cell has a total height of 400 mm and a rectangular cross section of 20 mm  $\times$  200 mm. It consists of lower (1) and upper (2) half cells arranged with one fixed upon the other. They can be separated (position a) or connected (position b) to start the diffusion by moving the sliding component (3) between the half cells by means of the magnets (9). The upper side of the slide marks the middle of the diffusion cell. Therefore, the volume (7) is part of the lower half cell and has to be filled with the same gas as this half cell. This is achieved by means of gushing pits (8) in the slide and in the lower cover plate (5). To avoid compression of the gas when the slide is

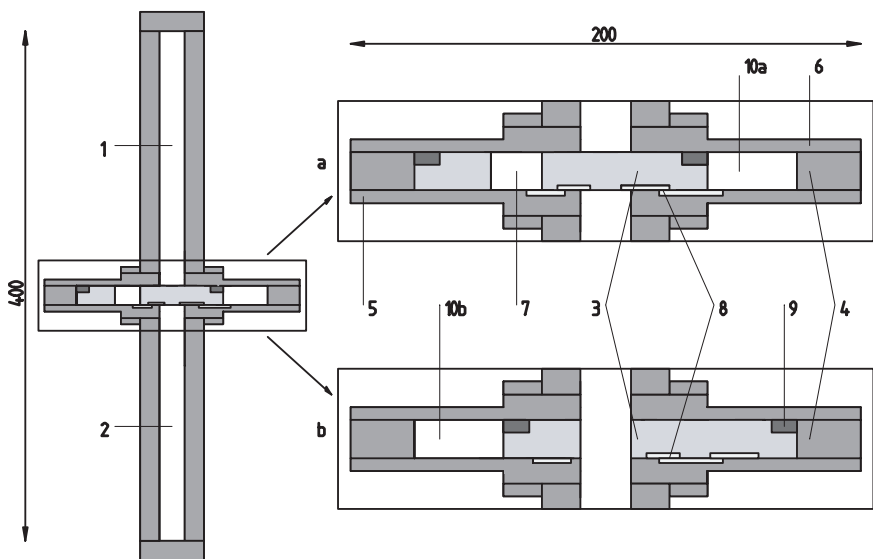


Fig. 3. Diffusion cell: (1) upper half cell, (2) lower half cell, (3) sliding component, (4) frame, (5) lower cover plate, (6) upper cover plate, (8) gushing pits, (9) magnets.

moved, the chamber (10a) is connected sideways with chamber (10b) by means of additional gushing pits not shown in the figure.

In order to meet the mechanical and magnetic requirements, non-magnetic steel X6CrNiTi18.10 was used as the material for the cell. All surfaces of the plates (5) and (6) and of the slide (3) were polished and afterwards coated with chromium nitride to increase the hardness of the surfaces and to avoid abrasions due to the movement of the slide.

The most important advantage in the construction of the new diffusion cell compared to common shearing cells is that both half cells are mounted with one fixed upon the other. Thus, only nonmoving parts of the cell have to be sealed and lubricants, which may dissolve the diffusing gases, are avoided.

Pairs of windows are mounted in both half cells for passing the laser beam. Acrylic glass has been chosen as the window material clamped by a steel frame and sealed by O-rings.

### 3.2. Pressure Control System

It is necessary to fill the separated half cells before the start of the diffusion with the corresponding gases simultaneously up to the pressure intended in the experiment. Pressure differences during and after the filling process would lead to convection and have to be avoided. For this purpose a pressure control system has been developed.

Unfortunately, tests have shown that the sliding component (3) (see Fig. 3) does not appropriately separate both half cells from each other so that one or even both gases could flow into the other half cell. Consequently, at least one of the half cells is not filled with a pure gas, but already with a gas mixture before the start of the diffusion. The composition at  $t=0$  in both half cells has to be known for the interferometric analysis and for the following determination of the diffusion coefficient.

### 3.3. Optical Arrangement

The Loschmidt cell is part of the optical setup for the holographic interferometer (Fig. 4). The beam of a He-Ne laser (1) passes to the first mirror (3) and is reflected to a beam splitter (4), where it can be split into the object and reference beams with variable intensity. Both coherent beams are widened to plane waves by the collimators (5). After passing the diffusion cell (6), the object wave interferes with the reference wave. The interference pattern before diffusion is stored photographically on a holographic plate (8) (Agfa 8E75 HD NAH) by exposing it to a short flash of light using an electronic shutter (2). In the diffusion experiment the

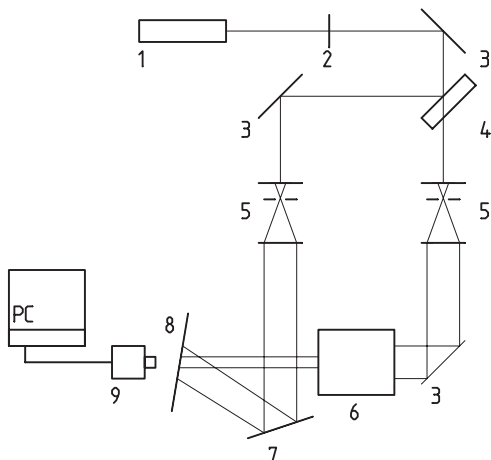


**Fig. 4.** Optical arrangement: (1) He-Ne-laser, (2) electronic shutter, (3) mirror, (4) beam splitter, (5) collimator, (6) diffusion cell, (7) piezo adjustable mirror, (8) holographic plate, (9) CCD matrix camera.

hologram is acting as a diffraction grating so that the original object wave can be created by the reference wave. The exact repositioning of the hologram is achieved by means of the piezo-driven adjustable mirror (7). After starting the diffusion, the current object wave interferes with the reconstructed object wave. This final interference pattern is recorded by a CCD matrix camera (9) and stored at definite time intervals (3 s) on a PC using a frame grabber board. The optical setup is arranged on an optical table equipped with a honeycomb structure and damping elements to reduce vibrations. The table is placed on four pillars passively air-damped, whereas the whole equipment is placed on a separate foundation.

Figure 2 shows interference patterns recorded by the CCD camera for (a) the beginning, (b) the intermediate, and (c) the further course of a diffusion experiment. As shown, only a small rectangular section in the middle of the windows is evaluated.

#### 4. RESULTS AND COMPARISON WITH LITERATURE DATA

The binary gas mixture Ar-C<sub>3</sub>H<sub>8</sub> was chosen as a test system. Both gases have similar molar masses and densities and differ sufficiently in refractive indices.

**Table I.** Coefficients of the Refractive Index as a Function of the Ideal Gas Density (see Eq. (24)) and Values of the First Refractivity Virial Coefficient for Argon and Propane

Gas Reference	$T$ (K)	$a_1$ (cm <sup>3</sup> ·mol <sup>-1</sup> )	$a_2$ (cm <sup>6</sup> ·mol <sup>-2</sup> )	$\delta \times 10^6$	$\mathcal{A}_i$ (cm <sup>3</sup> ·mol <sup>-1</sup> )
argon					
this work	294	6.44	—	1.4	4.29
Kerl and Häusler [7]	299	6.33	117	—	4.23
propane					
this work	294	24.22	6556	6.0	16.15
Kerl and Häusler [7]	299	24.16	9955	—	16.11

Refractive index measurements have been performed for argon and propane and have been evaluated using Eq. (24). In addition, the value of the first refractivity virial coefficient  $\mathcal{A}_i$  can be approximately calculated by

$$\mathcal{A}_i = \frac{2}{3} a_1 \quad (33)$$

The obtained values for  $a_1$ ,  $a_2$ ,  $\delta$ , and  $\mathcal{A}_i$  are shown in Table I.

In the beginning diffusion measurements were carried out at pressures from 1 to 5 bar at room temperature. Unfortunately, these measurements could not be evaluated properly because of the mixing of the pure gases during the filling process due to the imperfection of the sliding component. But additional test measurements showed that the gas flow via the sliding component occurred only in one direction so that the lower half cell was filled with pure propane. Therefore, the composition of the gas mixture in the upper half cell at  $t = 0$  could be calculated by means of its value at  $t \rightarrow \infty$ .

Finally, a measurement at  $p = 1$  bar and  $T = 294$  K was performed through the last interference fringe  $k_{\max}$ . A value of 107 was observed contrary to a calculated value  $k_{\max} = 115$  in the case of pure argon in the upper half cell at  $t = 0$ .

The values used for the pressure virial coefficients were taken from Dymond and Smith [8] and those for the optical coefficients from Kerl and Häusler [7]. Equations (4) to (6) were fitted separately to the obtained data of  $\rho_{C_3H_8}(z, t)$  and  $\rho_{Ar}(z, t)$ . The values resulting for  $D_{ij}\rho$  are shown in Fig. 5. The mean value resulting from this measurement is  $D_{ij}\rho = 4.33 \times 10^{-4} \text{ mol} \cdot \text{m}^{-1} \cdot \text{s}^{-1}$  with an uncertainty of  $\pm 1\%$ .

Diffusion measurements on the system Ar-C<sub>3</sub>H<sub>8</sub> are reported in three publications. A comparison of those results with the value of this work is given in Table II. Wakeham and Slater [9] used the Taylor dispersion

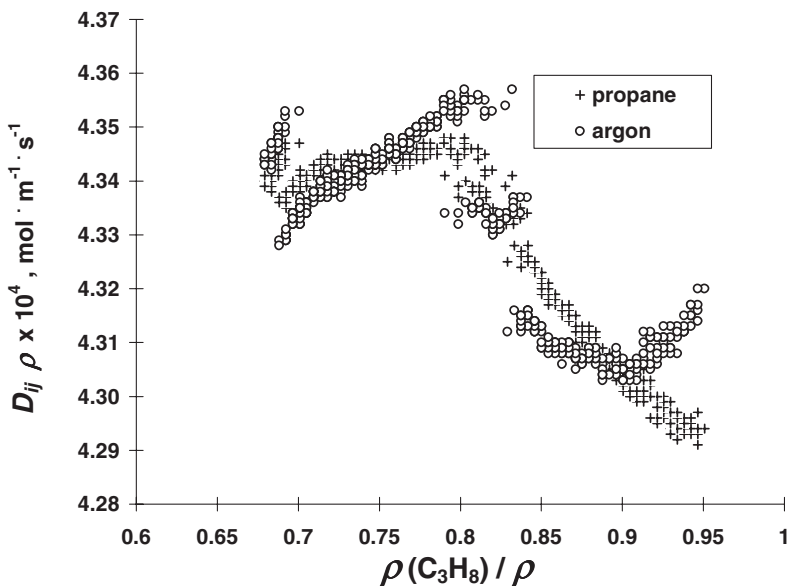


Fig. 5.  $D_{ij}\rho$  as a function of density of propane for the binary gas mixture Ar + C<sub>3</sub>H<sub>8</sub> at room temperature.

method to investigate the binary diffusion of traces of alkanes in argon at temperatures of 300 to 700 K. The value of  $D_{ij}\rho$  given in Table II was calculated using the density of argon and an extrapolated value of  $D_{ij}$  at  $T = 294$  K. Jacobs et al. [10] determined diffusion coefficients of methane, ethane, propane, and n-butane in N<sub>2</sub> and argon at  $T = 298$  K using a closed-tube technique different from a Loschmidt cell. The density of argon and a value of  $D_{ij}$  corrected to  $T = 294$  K were used to calculate  $D_{ij}\rho$ . Among others,  $D_{ij}$  for the argon + propane system was obtained by Lannus [11] at temperatures of 273 to 473 K with the two-bulb method.  $D_{ij}\rho$  was deduced using an interpolated value of  $D_{ij}$  at  $T = 294$  K and the mean density

Table II.  $D_{ij}\rho$  for the Binary Gas Mixture Ar + C<sub>3</sub>H<sub>8</sub> at 294 K

Reference	Method	$D\rho \times 10^4$ (mol · m <sup>-1</sup> · s <sup>-1</sup> )
this work	Loschmidt cell	4.33
Wakeham and Slater [9]	Taylor dispersion	4.30
Jacobs et al. [10]	closed-tube	3.61
Lannus [11]	two-bulb	4.59

$(\rho_{\text{Ar}} + \rho_{\text{C}_3\text{H}_8})/2$ . It has to be stressed that the deviations between the different data are larger than the uncertainty claimed by the authors. The value obtained in this work is in good agreement with the value of Wakeham and Slater.

## 5. CONCLUSION

A measuring system for the determination of binary diffusion coefficients has been developed. It consists of a Loschmidt cell improved with respect to lubricant-free tightness and a setup for holographic interferometry. This optical method makes it possible to determine the concentration changes over an extended range of the cell. Both half cells are filled simultaneously using a pressure control system. Since they could not be appropriately separated from each other, an undesired mixing of the gases during the filling process has occurred in the upper half cell. The composition of the gas mixture in the upper half cell at the start of the diffusion has been obtained by the determination of the composition at  $t \rightarrow \infty$ . A diffusion measurement on the system argon+propane has been carried out at  $p = 1$  bar and  $T = 294$  K and has been evaluated taking into account the mixing of gases during the filling process. Furthermore, refractive index measurements on the pure gases argon and propane as a function of gas density have been performed and evaluated to derive the first refractivity virial coefficient. The results of the diffusion experiment as well as of the refractive index measurements are in good agreement with literature values.

## REFERENCES

1. T. R. Marrero and E. A. Mason, *J. Phys. Chem. Ref. Data* **1**:3 (1972).
2. K. Kerl and M. Jescheck, *Z. Phys. Chem. (Frankfurt am Main)* **97**:127 (1975).
3. K. Kerl and M. Jescheck, *Int. J. Heat Mass Transfer* **26**:211 (1983).
4. S. F. Y. Li and W. A. Wakeham, in *Experimental Thermodynamics. Vol. III. Measurements of the Transport Properties of Fluids*, W. A. Wakeham, A. Nagashima, and J. V. Sengers, eds. (Blackwell Scientific, Oxford, 1991), p. 294.
5. J. Crank, *The Mathematics of Diffusion*, 2nd Ed. (Oxford Univ. Press, Oxford, 1975).
6. T. Kreis, *Holographic Interferometry: Principles and Methods* (Akademie Verl., Berlin, 1996).
7. K. Kerl and H. Häusler, *Ber. Bunsenges. Phys. Chem.* **88**:992 (1984).
8. J. H. Dymond and E. B. Smith, *The Virial Coefficients of Pure Gases and Mixtures: A Critical Compilation* (Clarendon Press, Oxford, 1980).
9. W. A. Wakeham and D. H. Slater, *J. Phys. B* **7**:297 (1974).
10. T. Jacobs, C. Peeters, and J. Vermont, *Bull. Soc. Chim. Belges* **79**:337 (1970).
11. A. Lannus *The Approximate Calculation of Diffusion Coefficients of Dilute Gases*, Ph.D. thesis (Drexel University, Philadelphia, 1970).